

**Strontium Titanate Perovskite SrTiO<sub>3</sub> as a Promising Ideal Material for  
MEMS Applications: First-principles FP-LMTO + LSDA Study**

**M. Musa Saad**

*Department of Physics, College of Science, Qassim University, Buridah 51452, Saudi Arabia*

*Mob: +966509353808; Fax: +966163800911, E-mail: musa.1964@gmail.com*

(Received 5/9/2013 - Accepted 28/11/2013)

**Abstract.** Strontium titanate perovskite oxide materials offer a number of advantages in micro-electromechanical systems (MEMS) due to the micro-structural, electronic, magnetic and mechanical properties. In this paper, we report theoretical study on structural, electronic, magnetic and mechanical properties of strontium titanate perovskite oxide SrTiO<sub>3</sub>. This material selected as energetic substrate primarily for its dimensional stability that is relatively insensitive to environment conditions. The calculations performed using the first-principles full-potential linear muffin-tin orbital (FP-LMTO) method, under the local spin density approximation (LSDA) and plus the on-site Coulomb interaction (LSDA+*U*) scheme. The analysis of densities of states, exchange interactions and magnetic moments reveals that SrTiO<sub>3</sub> exhibits a semiconductor character with an energy gap of  $E_g = 2.68$  eV, in excellent agreement with the previous experimental results.

**Keywords:** *MEMS material; Perovskite; Electronic properties; FP-LMTO method.*

## 1. Introduction

Transition-metal perovskite oxides (TMPO) are a huge family of inorganic materials that have been investigated extensively in the last decades due to their significance to fundamental research and their high potential for technological applications. These include used as dielectric materials in capacitors [1], oxygen ion semiconductors in sensors [2,3], substrates for high temperature superconductors [4], piezoelectric materials in actuators [5,6] electrodes in solid oxide fuel cell (SOFC) [7,8], etc. On the other hand, piezoceramic perovskite oxides are materials couple electrical and mechanical in stimulus-response manner. For example, when a mechanical force is applied, an electrical response arises which, in terms of voltage or charge, signal, is proportional to the magnitude of the applied stress. Conversely, when an electric field is applied, a mechanical stress or deformation or shape change develops. Ceramics are widely used for electromechanical sensors and actuators. Some examples of piezomaterials are crystalline quartz, barium titanate [9], vanadium niobate and lead zirconate titanate (PZT) [10].

In addition to, perovskites among the most important materials for a variety of applications, as well as, some of the most versatile for chemical tuning of composition and structure. Perovskite materials display a plethora of physical and chemical properties of technological interest that depend on processing conditions, oxygen content, and order. A thorough understanding of most of these properties requires the knowledge of the electronic structure of the bulk material. Materials that crystallize in TMPO structure have the general formula of  $AMO_3$ . Strontium titanate  $SrTiO_3$  is one of the most important oxide materials because of its potential to be used in dielectric and optical devices, as well as, used as substrate material for superconducting thin films.  $SrTiO_3$  is typical perovskite-type compounds with band energy of about 3.2 eV [1,9]. The electronic structure of doped, such Nb-doped  $SrTiO_3$ , and un-doped  $SrTiO_3$  has been reported in several experimental and theoretical studies. In fact, a lot of theoretical calculations of electronic band structures have been performed on  $SrTiO_3$ . In the present study we deal with the structural, electronic, magnetic and mechanical properties of  $SrTiO_3$ .

## 2. Computational details

In this study, first-principles self-consistent band structure calculations were performed by using full potential linear muffin-tin orbital (FP-LMTO) method within atomic plane wave (PLW) representation [11], as implemented in the available computer code LmtArt [12]. In FP-LMTO method, there is no shape approximation to the crystal potential; the crystal is divided up into two regions; inside muffin-tin spheres (MTSs), where Schrödinger's equation is solved numerically, and an interstitial region (IR), where the wave-functions are Hankel functions [13-15]. The key-point in this method, the potential ( $V_{MT}$ ) inside MTSs ( $r \leq S_{MT}$ ) is assumed to be spherically symmetric close to the ion-core, while in IR ( $r > S_{MT}$ ), it is assumed to be flat in between, thus,  $V_{MT}$  can be represent as:

$$V_{MT}(r) = \begin{cases} V(r); & (r \leq S_{MT}) \\ V_{MTZ}; & (r > S_{MT}) \end{cases} \quad (1)$$

Where,  $S_{MT}$  is the radius of the MTS, and  $r$  is a position.

Inside MTSs, the basis sets are described by the solution of the radial Schrödinger's equation of fixed energy and multiplied by spherical harmonics [11,13], as:

$$\left[ \frac{d^2}{dr^2} - V(r) + \frac{l(l+1)}{r^2} - E \right] r \phi_l(r, E) = 0 \quad (2)$$

In IR, the basis set consists of plane-waves, described by the Hankel function  $h_{\kappa l}^{(1)}(r) = h_{\kappa l}^{(1)}(r) i^l Y_{lm}(r)$  of energy  $\kappa^2$  [12,13].

The exchange correlation energy of electrons is described in the local spin density approximation (LSDA) technique, in the framework of density functional theory (DFT), employed by using the parameterization of Barth-Hedin version [16]. The electron-electron interaction energy for the localized (strong correlated)  $d$  states in LSDA depends only on the total number of localized electrons  $n_d = \sum_i n_i$ , with  $n_i$  being the orbital occupancies of the localized states [17]. The exchange correlation energy is:

$$E_{XC}^{LSDA}[n \uparrow, n \downarrow] = \int \varepsilon_{XC}(n \uparrow, n \downarrow) n(r) d^3 r \quad (3)$$

Where,  $\varepsilon_{xc}$  is the exchange-correlation energy as a function of spin-up  $n(r)\uparrow$  and spin-down  $n(r)\downarrow$ , with a total spin-density of states of  $n(r) = n(r)\uparrow + n(r)\downarrow$ .

To treat strong electron interactions effect in Ti (3d), the LSDA+ $U$  calculations have been carried out in the Hubbard model framework [17].

$$E_{XC}^{LSDA+U}[n \uparrow, n \downarrow] = E_{XC}^{LSDA}[n \uparrow, n \downarrow] + E_{XC}^U[n \uparrow, n \downarrow] \quad (4)$$

The Hubbard repulsion energy is:

$$E_{XC}^U[n \uparrow, n \downarrow] = \frac{U - J}{2} \sum_i \sum_{m\sigma} n_{m\sigma}^i (1 - n_{m\sigma}^i) \quad (5)$$

Where,  $n_{m\sigma}^i$  is the spin  $\sigma$  and orbital  $m$  occupation numbers for  $I$  site.

In this work, by means of the option of  $U = 3.0$  eV and the exchange parameter  $J = 0.89$  eV for strongly correlated Ti (3d) electrons [18]. For correct description of the wave functions in the interstitial region, the spherical harmonics is

expanded up to the value of  $l_{\max} = 6$  for Sr, Ti, and O MTSS. The Brillouin zone (BZ) integration in the course of the self-consistency iterations was performed over a  $(6 \times 6 \times 6)$  mesh with 50  $k$ -points in the irreducible part of the BZ. Single kappa ( $\kappa = 1$ ) *spdf* LMTOs basis is used, each radial function inside the spheres is matched to a Hankel function in the interstitial region, for describing the valence bands [19].

In order to obtain better results of DOSs, the correlation parameters, the Coulomb repulsion ( $U$ ) and Hund's rule exchange ( $J$ ), were utilized for correlated  $d$ -electrons. For 3d, 4d and 5d electrons, only three effective Slater integrals  $F^0$ ,  $F^2$  and  $F^4$  (in  $Ry$  units;  $eV \approx 0.0735 Ry$ ) require being determined for FP-LMTO [12-13]. The relationships between the Slater integrals and the parameters  $U$  and  $J$  can be expressed in the formulas, as [14]:

$$F^0 = U, F^2 = \frac{14}{1.625}J, F^4 = 0.625F^2 \quad (6)$$

### 3. Results and Discussion

The crystal structure parameters are calculated by using the SpuDS (Structure Prediction Diagnostic Software) [20].  $SrTiO_3$  has an ideal cubic crystal structure with space group of Pm-3m (No. 221), with lattice parameter of about  $a_0 = 3.93 \text{ \AA}$  and unit cell volume of  $V = 60.701 \text{ \AA}^3$ , at room-temperature (RT), agreement with the previous values [21-24], see Table 1. The atomic positions in the elementary cell are Sr (1b) at the corners of the cube  $(1/2, 1/2, 1/2)$ , Ti (1a) at the center  $(0, 0, 0)$ , and O (3d) at the face-centered positions  $(1/2, 0, 0)$ ,  $(0, 1/2, 0)$  and  $(0, 0, 1/2)$ , see Fig. (1).

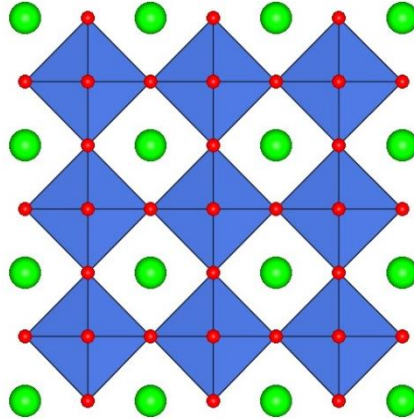


Fig (1). 3D Representation of crystal structure of cubic  $SrTiO_3$  with space group of (Pm-3m), Sr (green spheres), Ti (in the center of 4ferromagne  $TiO_6$ ) and O (small red spheres).

Additional physical properties of SrTiO<sub>3</sub>, such thermal expansion, deformation, mass-density and hardness have been investigated. The effect of temperature on the lattice shape; the lattice parameter, volume and interatomic distances are calculated systemically. As seen in Fig. (2), it found that there are small expansion occurs dramatically in [Ti – O] and [Sr – O] bond distances due to change in temperature. The coefficient of thermal expansion has been calculated and found to be  $1.6804 \times 10^{-5}$  ( $\text{\AA}/^\circ\text{C}$ ), thus, the stress occurs is three dimensions. Therefore, the dimensional stability of SrTiO<sub>3</sub> is high, which is relatively insensitive to environmental conditions, such temperature or stress.

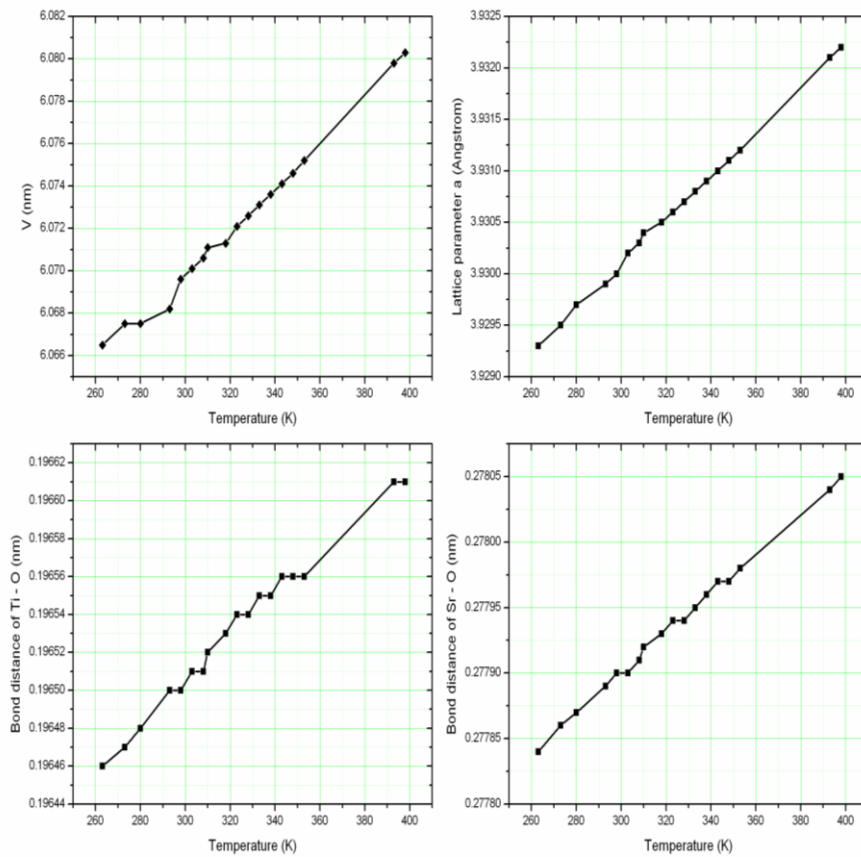


Fig. (2). Volume, lattice parameter, bond-distances of SrTiO<sub>3</sub> as functions of temperature

The electronic structure of  $\text{SrTiO}_3$  is calculated within the LSDA and LSDA+ $U$  methods. Figs. (3 and 4) show the calculated total and partial densities of states (DOS) of  $\text{SrTiO}_3$ . The calculation for the perfect structure presents the ground state to be semiconducting character with energy gap of about  $E_g = 2.68$  eV. The total DOS obviously evidences that the two spin channels show an energy gap in the conduction region (0.0 eV – 1.65 eV) and (0.0 eV – 1.07 eV) in LSDA and LSDA+ $U$  results, respectively. The energy gap locates between the  $t_{2g}$  spin-up and spin-down of Ti (3d) mediated with O (2p) sub-bands. This attributes to the superexchange interaction Ti (3d) – O (2p) – Ti (3d) mechanism.

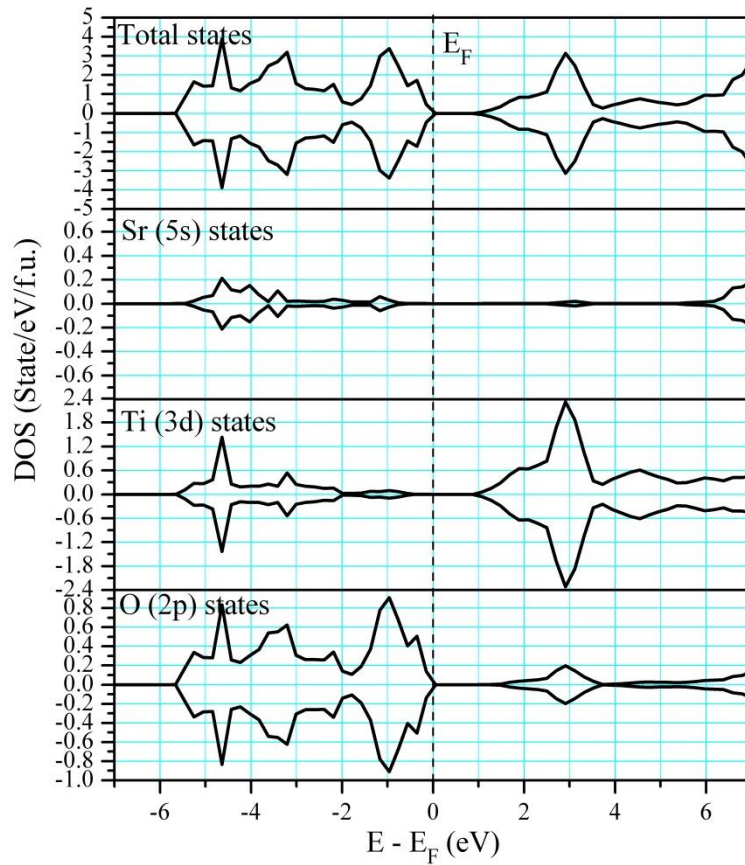


Fig. (3). Total and partial densities of states of  $\text{SrTiO}_3$  from LSDA ( $U = 0$  eV), Fermi level is sited at ( $E_F = 0$ ).

The LSDA and LSDA+*U* calculations of partial and total magnetic moments of SrTiO<sub>3</sub> are:  $-0.1226\text{E-}6 \mu_B$  for Ti (3d), which has the ionic configuration of Ti<sup>4+</sup> (3d<sup>0</sup>; t<sub>2g</sub><sup>0</sup>, *S* = 0) and is polarized antiferromagnetically. For Sr (5s) and O (2p), are  $0.1051\text{E-}8 \mu_B$  and  $0.451\text{E-}7 \mu_B$ , respectively, yield a total magnetic moment of  $-0.7645\text{E-}7 \mu_B$ , approximately zero ( $m = 0.0 \mu_B$ ). As a result, in the simple ionic model, the titanium ion in SrTiO<sub>3</sub> is tetravalent and has no 3d electrons Ti<sup>4+</sup> (3d<sup>0</sup>). Since there are no 3d electrons nominally that being appreciable correlation interactions, the electronic structure of SrTiO<sub>3</sub> is possibly describe by the energy-band picture. In SrTiO<sub>3</sub>, Figs. (3 and 4), the top of valence band (VB) is mainly composed of O (2p) states and the bottom of the conduction band (CB) is formed by the Ti (3d) states. However, it is known that the Ti (3d) orbital electrons are strongly hybridized with those in O (2p). This leads to the situation in which non-vanishing 3d electrons exist in the ground state.

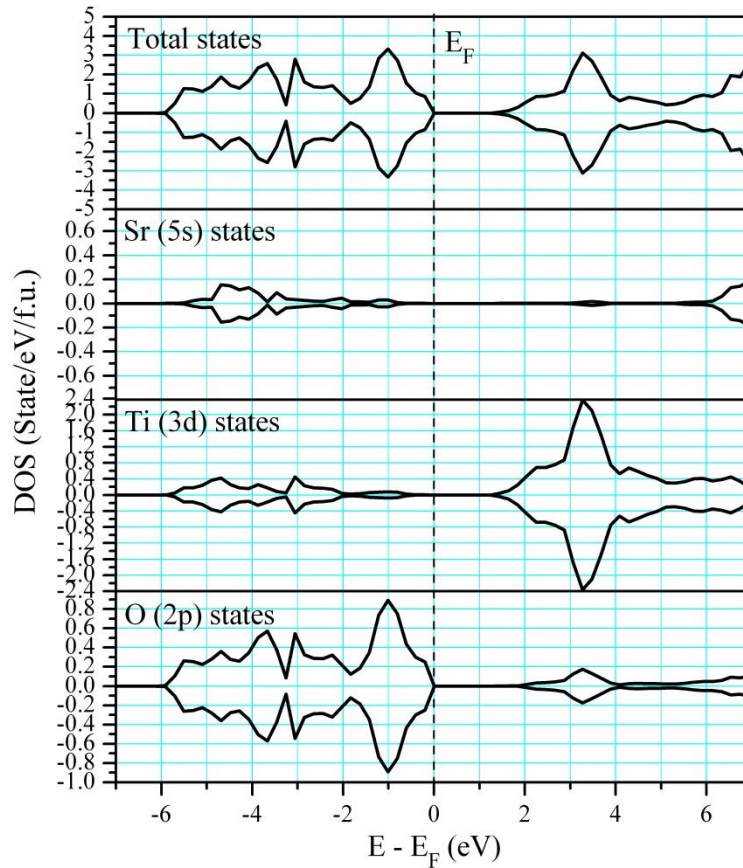


Fig. (4). Total and partial densities of states of SrTiO<sub>3</sub> from LSDA (*U* = 6.0 eV), Fermi level is sited at ( $E_F = 0$ ).

**Table (1).** Calculated values for the lattice constants ( $a_0$ ), unit cell volumes ( $V$ ), bulk modulus ( $B$ ), valence bandwidths ( $\Delta W_V$ ) and band gaps ( $E_g$ ) for the cubic perovskite SrTiO<sub>3</sub> in comparison with available experimental and theoretical data.

Parameters	This work	Exp.	Theo.
$A_0$ (Å)	3.93	3.92 <sup>a</sup> , 3.90 <sup>b</sup>	3.94 <sup>c</sup> , 3.95 <sup>a</sup>
$V$ (Å <sup>3</sup> )	60.701	59.547 <sup>d</sup>	57.067 <sup>e</sup> , 58.141 <sup>f</sup>
$B_0$ (Gpa)	169.43	169.0 <sup>a</sup>	169.72 <sup>c</sup> , 170.0 <sup>g</sup>
$\Delta W_V$ (eV)	5.56	3.79 <sup>a</sup>	5.0 <sup>h</sup>
$E_g$ (eV)	2.68	3.2 <sup>h</sup>	2.71 <sup>k</sup> , 3.57 <sup>a</sup>

*a* Ref. [21], *b* Ref. [22], *c* Ref. [23], *d* Ref. [24], *e* Ref. [25], *f* Ref. [26], *g* Ref. [27], *h* Ref. [28], *k* Ref. [29].

Strontium titanate perovskite oxide SrTiO<sub>3</sub> can be used as substrate material for MEMS applications. The popularity of SrTiO<sub>3</sub> for such application is primarily for the following reasons:

1. SrTiO<sub>3</sub> is mechanically stable and it can be integrated into electronics on the same substrate. Electronics for signal transduction, such as a p- or n-type piezoresistor, can be readily integrated with the perovskites substrate.

2. SrTiO<sub>3</sub> has a high Young's modulus; materials with a high Y can better maintain a linear relationship between applied load and the induced deformations.

3. SrTiO<sub>3</sub> has high melting points, at 2080 °C; this high melting point makes perovskites dimensionally stable even at elevated temperature.

4. Its thermal expansion coefficient is smaller than that of some metals, such steel and aluminum.

5. SrTiO<sub>3</sub> is an ideal semiconductor with small energy-gap at room temperature.

Above all, the perovskite oxide SrTiO<sub>3</sub> shows virtually no mechanical hysteresis. It is thus an ideal candidate material for sensors and actuators applications. Moreover, perovskite oxide wafers are extremely flat and accept coatings and additional thin-film layers for building micro-structural geometry or conducting electricity. Moreover, there is a greater flexibility in design and manufacture with perovskite oxides, similar to silicon, than with other substrate materials. Treatments and fabrication processes for perovskite oxide substrates are well established and documented.

#### 4. Conclusion

In summary, the structural, electronic, magnetic and mechanical properties of strontium titanate perovskite oxide SrTiO<sub>3</sub> were studied by using the first-principles full-potential linear muffin-tin orbital (FP-LMTO) method, under the local spin



density approximation (LSDA) and plus the on-site Coulomb interaction (LSDA+*U*) scheme. It is found that the SrTiO<sub>3</sub> perovskite oxide materials offer a number of advantages in micro-electromechanical systems (MEMS) due to the structural, electronic, magnetic and mechanical properties. SrTiO<sub>3</sub> material is selected as energetic substrate primarily for its dimensional stability that is relatively insensitive to environment conditions. The analysis of DOS, exchange interactions and magnetic moments revealed that SrTiO<sub>3</sub> exhibits a semiconductor character with an energy gap of  $E_g = 2.68$  eV. The results and characters demonstrated the promising applications of an ideal SrTiO<sub>3</sub> in sensors and actuators and other MEMS technology.

### References

- [1] Michael Biegalski, Susan Trolier-McKinstry, "Modeling Optical Changes in Perovskite Capacitor Materials Due to dc-Field Degradation", *J. American Ceramic Soc.* 88, (2005), 71–78.
- [2] Jeffrey W. Fergus, "Perovskite oxides for semiconductor-based gas sensors", *Sensors and Actuators B: Chemical* 123, (2007), 1169–1179
- [3] Koduri Ramam, A. J. Bell, C. R. Bowen, K. Chandramouli, "Investigation of dielectric and piezoelectric properties of niobium-modified PLSZFT nanoceramics for sensor and actuator applications", *J. Alloy. Compd.* 473, (2009), 330 – 335.
- [4] J. Paul Attfield, "Chemistry and high temperature superconductivity", *J. Mater. Chem.* 21, (2011), 4756 – 4764.
- [5] S. Halder, P. Gerber, T. Schneller, R. Waser, "Electromechanical properties of Ba(Ti<sub>1-x</sub>Zr<sub>x</sub>)O<sub>3</sub> thin films", *Appl. Phys. A* 81, (2005), 11– 13.
- [6] RenZheng Chen, AiLi Cui, XiaoHui Wang, ZhiLun Gui, LongTu Li, "Structure, sintering behavior and dielectric properties of silica-coated BaTiO<sub>3</sub>", *Mater. Lett.* 54, (2002), 314 – 317.
- [7] Stephen J. Skinner, "Recent advances in Perovskite-type materials for solid oxide fuel cell cathodes", *International J. Inorganic Mater.* 3, (2001), 113 – 121.
- [8] J. Peña-Martínez, D. Marrero-López, J.C. Ruiz-Morales, B.E. Buegler, P. Núñez, L. J. Gauckler, "Fuel cell studies of perovskite-type materials for IT-SOFC", *J. Power Sources* 159, (2006), 914 – 921.
- [9] R. Ahuja<sup>1</sup>, O. Eriksson<sup>1</sup>, B. Johansson, "Electronic and optical properties of BaTiO<sub>3</sub> and SrTiO<sub>3</sub>", *J. Appl. Phys.* 90, (2001), 1854.
- [10] J Frantti, Y Fujioka, R M Nieminen, "Evidence against the polarization rotation model of piezoelectric perovskites at the morphotropic phase boundary", *J. Phys.: Condens. Matter* 20, (2008), 472203.

- [11] S. Yu. Savrasov, D. Y. Savrasov, “Full-potential linear-muffin-tin-orbital method for calculating total energies and forces”, *Phys. Rev. B* 46, (1992), 12181 – 12195.
- [12] I. V. Solovyev, “Electronic structure and stability of the ferromagnetic ordering in double perovskites”, *Phys. Rev. B* 65, (2002), 144446.
- [13] S. Y. Savrasov, “Linear-response theory and lattice dynamics: A muffin-tin-orbital approach”, *Phys. Rev. B* 54, (1996), 16470.
- [14] O. Miura and T. Fujiwara, “Electronic structure and effects of dynamical electron correlation in ferromagnetic bcc Fe, fcc Ni, and antiferromagnetic NiO”, *J. Phys. Rev. B* 77, 195124 (2008).
- [15] I. Di Marco, J. Minar, S. Chadov, M. I. Katsnelson, H. Ebert, A. I. Lichtenstein, “Correlation effects in the total energy, the bulk modulus, and the lattice constant of a transition metal: Combined local-density approximation and dynamical mean-field theory applied to Ni and Mn”, *Phys. Rev. B* 79, 115111 (2009), 1-14.
- [16] U. von Barth, L. Hedin, “A local exchange-correlation potential for the spin polarized case”, *J. Phys. C: Solid State Phys.* 5 (13), (1972) 1629-1642.
- [17] Antonis N. Andriotis, R. Michael Sheetz, Madhu Menon, “LSDA+ $U$  method: A calculation of the  $U$  values at the Hartree-Fock level of approximation”, *Phys. Rev. B* 81, 245103, (2010), 1 –5.
- [18] J. P. Zhou, R. Dass, H. Q. Yin, J.-S. Zhou, L. Rabenberg, J. B. Goodenough, “Enhancement of room temperature magnetoresistance in double perovskite ferrimagnets”, *J. Appl. Phys.* 87, 5037, (2000).
- [19] M. Methfessel, C. O. Rodriguez, O. K. Andersen, “Fast full-potential calculations with a converged basis of atom-centered linear muffin-tin orbitals: Structural and dynamic properties of silicon”, *Phys. Rev. B* 40, (1989), 2009-2012.
- [20] M. W. Lufaso, P. M. Woodward, “Prediction of the crystal structures of perovskites using the software program SpuDS”, *Acta Cryst. B: Struct. Sci.* 57, (2001), 725 – 733.
- [21] S. Piskunov, E. Heifets, R.I. Eglitis, G. Borstel, “Bulk properties and electronic structure of SrTiO<sub>3</sub>, BaTiO<sub>3</sub>, PbTiO<sub>3</sub> perovskites: an ab initio HF/DFT study”, *Comput. Mater. Sci.* 29, (2004), 165.
- [22] Y. A. Abramov, V. G. Tsirelson, “The chemical bond and atomic displacements in SrTiO<sub>3</sub> from X-ray diffraction analysis”, *Acta Cryst. B* 51(6), (1995), 942 – 951.
- [23] A. Boudali, M. Driss Khodja, B. Amrani, D. Bourbie, K. Amara, A. Abada, “First-principles study of structural, elastic, electronic, and thermal properties of LaAlO<sub>3</sub> perovskite”, *Phys. Lett. A* 373, (2009), 879 – 884.

- [24] O. Nakagawara, M. Kobayashi, Y. Yoshino, Y. Katayama, H. Tabata, T. Kawai, "Effects of buffer layers in epitaxial growth of SrTiO<sub>3</sub> thin film on Si(100)", *J. Appl. Phys.* 78, 7226, (1995).
- [25] K. Johnston, M. R. Castell, A. T. Paxton, M. W. Finnis, "SrTiO<sub>3</sub>(001)(2×1) reconstructions: First-principles calculations of surface energy and atomic structure compared with scanning tunneling microscopy images", *Phys. Rev. B* 70,085415, (2004), 1 – 12.
- [26] J. Junquera, M. Zimmer, P. Ordejon, P. Ghosez, "First-principles calculation of the band offset at BaO/BaTiO<sub>3</sub> and SrO/SrTiO<sub>3</sub> interfaces", *Phys. Rev. B* 67, 155327, (2003).
- [27] R. O. Bell, G. Rupprecht, "Elastic Constants of Strontium Titanate", *Phys. Rev.* 129, 90, (1963).
- [28] T. A. Noland, "Optical absorption of single-crystal strontium titanate", *Phys. Rev.* 94, 724, (1954).
- [29] Davide Ricci, Giuseppe Bano, Gianfranco Pacchioni, "Electronic structure of a neutral oxygen vacancy in SrTiO<sub>3</sub>", *Phys. Rev. B* 68, 224105, (2003).

بيروفسكيت تيتانات السترونتيوم  $SrTiO_3$  كمادة مثالية واعدة لتطبيقات أنظمة  
الكهروميكانيكية الدقيقة MEMS: دراسة باستخدام المبادئ الأولية  
FP-LMTO + LSDA

محمد موسى سعد

قسم الفيزياء، كلية العلوم، جامعة القصيم، بريدة ٥١٤٥٢، المملكة العربية السعودية  
(قدم في ٢٠١٣/٩/٥ م - وقيل في ٢٠١٣/١١/٢٨ م)

ملخص البحث. مواد أكسيد البيروفسكيت من تيتانات السترونتيوم تقدم عددا من المزايا التي تجعلها مناسبة لاستخدامها في أنظمة الكهروميكانيكية الدقيقة (MEMS) نظرا لخصائصها التركيبية، الإلكترونية، المغناطيسية والميكانيكية. في هذه الورقة، نحن نقدم تقريرا على الدراسة النظرية للخصائص التركيبية، الإلكترونية، المغناطيسية والميكانيكية لأكسيد البيروفسكيت من تيتانات السترونتيوم  $SrTiO_3$ . هذه المادة اختيرت كركيزة حيوية في المقام الأول لاستقرار أبعادها فهي حساسة نسبيا للظروف البيئة المحيطة. تم إجراء العمليات الحسابية باستخدام المبادئ الأولية لطريقة الجهد الكلي الخطي الكعكي المداري (FP-LMTO) ، تحت أسلوب التقريب كثافة السبين المحلية بالإضافة إلى تفاعل كولومب في طريقة (LSDA+U) . تحليل نتائج كثافة الحالات، التفاعلات التبادلية والعزم المغناطيسي يكشف عن أن  $SrTiO_3$  يسلك طابع أشباه الموصلات مع وجود فجوة طاقة مقدارها ٦٨.٢ إلكترون-فولت، في اتفاق ممتاز مع النتائج التجريبية السابقة.